Chemical Engineering Journal 166 (2011) 454–459

Contents lists available at ScienceDirect

Chemical Engineering Journal

journal homepage: www.elsevier.com/locate/cej

Adsorption of copper on amine-functionalized SBA-15 prepared by co-condensation: Kinetics properties

Enshirah Da'na [a], Nimal De Silva [b], Abdelhamid Sayari [a,c,*]

[a] Department of Chemical and Biological Engineering, University of Ottawa, Ottawa, Ontario K1N 6N5, Canada
[b] Department of Earth Science, University of Ottawa, Ottawa, Ontario K1N 6N5, Canada
[c] Department of Chemistry, University of Ottawa, Ottawa, Ontario K1N 6N5, Canada

ARTICLE INFO

Article history:
Received 3 September 2010
Received in revised form 4 November 2010
Accepted 4 November 2010

Keywords:
Heavy metals removal
Mesoporous silica
Amine-functionalized SBA-15
Adsorption
Co-condensation
Kinetics

ABSTRACT

Amino-functionalized SBA-15 prepared by co-condensation was tested for the removal of copper ions from aqueous solutions under different temperatures, pH, initial concentrations and agitation speeds. The obtained results indicated that the amino-functionalized SBA-15 was very efficient and equilibrium was achieved in less than 30 min at room temperature. The kinetic data was analyzed using four models, namely the first-order, the pseudo first- and second-order and the intraparticle diffusion model. Within the conditions used, the pseudo second-order kinetic model provided the best fit to the experimental data. Applying the intraparticle model showed that the adsorption involved three different stages.

1. Introduction

Similar to other heavy metals, copper enters the ecosystem through many processes including mining and refining, agricultural operations and industrial effluents, such as tanning processes, timber production, and electroplating industries. The release of large quantities of copper into the natural environment represents a serious threat to human health and other living species as well as ecological systems [1]. Therefore, efficient removal of copper from wastewater by appropriate treatments has long been a crucial issue. Adsorption is an attractive option because it is a simple, cost effective, and reversible process.

With the increasing demand for economical large-scale water treatment facilities, the development of efficient adsorbents for the removal of heavy metals that exhibit fast kinetics at high flow rates would be of great significance. A wide range of conventional porous solids, such as clay, fly ash, activated carbon and silica materials have attracted attention because of their relatively low-cost [2]. However, such materials have non uniform pore structures and often low adsorption capacities with slow adsorption kinetics [3]. Thus, the ideal adsorbent should have a stable and accessible pore structure with uniform pore size distribution as well as high surface area. Periodic mesoporous SBA-15 silica has many attractive characteristics such as large surface area, high porosity, controllable and narrowly distributed pore sizes, and an ordered pore arrangement. In addition, SBA-15 has some of the largest mesopores (5–30 nm), which allow unhindered accessibility of the internal surface of the material, leading to fast kinetics of chemical or physical processes. Furthermore, its thick pore walls of around 4 nm, provide enhanced mechanical stability. Recently, many authors anchored functional groups on the surface of SBA-15 using post-synthesis procedures [4–7] or co-condensation [7–11], some of which were reported to be very efficient for the adsorption of heavy metals from water [6,9–11].

The kinetics of adsorption, which dictates the residence time of the adsorption, is one of the most important tools to assess the adsorption efficiency. Therefore, it is important to be able to predict the rate of copper adsorption as a key step to design appropriate treatment units. In addition, investigating the copper adsorption kinetics is significant as it provides valuable insights into the reaction pathways. Walcarius and Delacôte investigated the effect of structural and surface properties of organically modified silicates on the kinetics of mercury adsorption [12]. Furthermore, Aguado et al. studied the effect of initial copper concentration on the adsorption kinetics of amine-functionalized SBA-15 prepared by grafting [7]. However, the effects of other factors such as temperature, pH, and agitation speed on the kinetics of metal removal by surface-functionalized SBA-15 has not been addressed. Hence, the goal of this work was to carry out an in-depth study on the effect of adsorption process parameters such as temperature, copper concentration, stirring speed, and pH on the performance of

* Corresponding author at: Department of Chemistry, University of Ottawa, Ottawa, Ontario K1N 6N5, Canada.
E-mail address: abdel.sayari@uottawa.ca (A. Sayari).

1385-8947/$ – see front matter © 2010 Elsevier B.V. All rights reserved.
doi:10.1016/j.cej.2010.11.017

the amine-modified SBA-15 obtained by co-condensation. Furthermore, this work dealt with the development of general predictive models to describe the relationship between the initial concentration and the adsorption temperature with the rate of copper removal.

2. Materials and methods

2.1. Adsorbent synthesis and characterization

Details of adsorbent synthesis and characterization can be found in an earlier contribution [11]. Briefly, 4.0 g of P123 and 8 g KCl were dissolved in 30 mL of water and 120 mL of a 2 M HCl solution at 40 °C. Then, 8.5 g of tetraethylorthosilicate was added and prehydrolyzed for 2 h before adding 1.08 g of 3-aminopropyltrimethoxy-silane (APTS). The mixture was stirred for 20 h, then heated at 100 °C for 24 h in static conditions. The material was collected by filtration, dried in air at room temperature and then extracted with ethanol. The material was further treated in aqueous 0.1 M HCl for 1 h and neutralized in 0.1 M $NaHCO_3$, then filtered and dried under vacuum at 100 °C for 3 h. The material will be referred to as APTS-SBA-15-AB.

2.2. Adsorption kinetics

Batch kinetic tests were performed in a 1 L glass reactor stirred at a specified rate (100 or 300 rpm) using a magnetic stirrer. The reactor was immersed in a water bath maintained at a constant temperature of 293, 313 or 333 K. The reaction mixture consisted of a total 1 L volume of 20, 100, or 200 ppm copper solution containing 1.0 g of adsorbent and the pH was adjusted at 5.5, 6.0, or 6.5. The reactor was coupled with an ICP-OES Varian Vista-Pro CCD spectrometer instrument for real-time measurement of copper concentration at intervals of 20 s for 2 h. The adsorption rate, defined as the change of copper concentration with time, was analyzed using the following models:

2.2.1. First-order model

For the first order kinetic, the adsorption of copper from liquid phase to solid phase may be expressed as:

$$A \underset{k_2}{\overset{k_1}{\rightleftharpoons}} B \tag{1}$$

where A is copper in solution, B is the adsorbed copper, k_1 and k_2 are the adsorption and desorption rate constants (h^{-1}). If C_0 is the initial concentration of copper ($mg\,L^{-1}$) and X the amount transferred from liquid phase to solid phase ($mg\,L^{-1}$) at any time t, then the rate can be expressed as:

$$\frac{dX}{dt} = k_1(C_0 - X) - k_2X \tag{2}$$

If X_e represents the concentration of copper adsorbed at equilibrium ($mg\,L^{-1}$), then,

$$-\ln\left(1 - \frac{X}{X_e}\right) = (k_1 + k_2)\,t \tag{3}$$

Further, the overall rate constant k (h^{-1}) is given by:

$$k = (k_1 + k_2) \tag{4}$$

Using the kinetic equation, the overall rate constant (k) can be calculated by plotting $\ln\left(1 - \frac{X}{Xe}\right)$ versus t.

2.2.2. Pseudo first-order model

The pseudo first-order kinetic model is based on the assumption that the adsorption rate is proportional to the number of free sites. The rate constant of adsorption can be determined using the following rate expression:

$$\frac{dq}{dt} = k_{p1}(q_e - q_t) \tag{5}$$

where q_t and q_e are the amounts of copper adsorbed ($mg\,g^{-1}$) at time t and at equilibrium, respectively. Integration and rearrangement of Eq. (5) gives:

$$\ln(q_e - q_t) = \ln q_e - k_{p1}t \tag{6}$$

k_{p1} is the pseudo first-order rate constant for adsorption (h^{-1}) and can be calculated from the slope of the linear plot of $\ln(q_e - q_t)$ versus t.

2.2.3. Pseudo second-order model

Pseudo second-order model is based on the assumption that the adsorption rate is linearly related to the square of the number of unoccupied sites, and thus the kinetic rate law can be written as follows:

$$\frac{dq}{dt} = k_{p2}(q_e - q_t)^2 \tag{7}$$

The differential equation is usually integrated and transformed in its linear form.

$$\frac{t}{q_t} = \frac{1}{k_{p2}q_e^2} + \frac{1}{q_e}t \tag{8}$$

where k_{p2} is the pseudo second-order rate constant for adsorption (g/mmol min) and can be determined by plotting t/q_t versus t.

2.2.4. Intraparticle diffusion model

The adsorbate transport from the solution phase to the surface of the adsorbent particles occurs in several steps. The overall adsorption process may be influenced by one or more steps, e.g. film or external diffusion, pore diffusion, and adsorption on the pore surface. A process is diffusion-controlled when its rate depends upon the rate at which diffusion takes place. The possibility of intraparticle diffusion will be explored using the intraparticle diffusion model:

$$q_t = k_{id}t^{1/2} \tag{9}$$

where k_{id} is the rate constant for intraparticle diffusion ($mg\,g^{-1}\,h^{-0.5}$). If the plot of q_t versus $t^{0.5}$ gives a straight line, then the adsorption process is controlled by intraparticle diffusion only. However, if the data exhibit multi-linear plots, then two or more steps influence the adsorption process [13–14].

3. Results

3.1. Effect of initial concentration

The copper uptake versus time at 333 K was measured for three different initial concentrations of Cu^{2+} ions, namely 20, 100 and 200 ppm. The curves in Fig. 1 show that initially, the amount of copper ions adsorbed increases significantly with time, then slows down gradually until the equilibrium is reached. This is mainly because initially most of the external and easy accessible sites were available and the copper concentration gradient was high. As the time passes the extent of copper adsorption decreases significantly because the number of vacant sites as well as the concentration gradient decrease. Fig. 1 shows the effect of initial concentration on adsorption kinetics, and Table 1 summarizes the calculated parameters for each initial copper concentration. Regression coefficients (R^2) obtained from the linear fits indicate good correlation for the three concentrations with the pseudo second-order model,

Table 1
Effect of experimental conditions on Cu^{2+} adsorption kinetics.

T (K)	pH	C_0 (ppm)	Agitation (rpm)	q_e (mmol/g)	q_{exp} (mmol/g)	K_{p2} (g/mmol min)	R^2	K_{id} (mmol/g $min^{0.5}$)
293	6.0	100	300	0.180	0.182	11.793	0.995	0.036
313	6.0	100	300	0.415	0.438	1.957	0.996	0.048
333	6.0	100	300	0.676	0.688	0.471	0.998	0.076
333	5.5	100	300	0.632	0.656	2.111	0.995	0.080
293	6.5	100	300	0.566	0.584	0.359	0.994	0.052
333	6.0	200	300	1.077	1.118	0.293	0.996	0.151
333	6.0	20	300	0.314	0.311	6.195	0.999	0.063
333	6.0	100	100	0.672	0.680	0.445	0.994	0.073

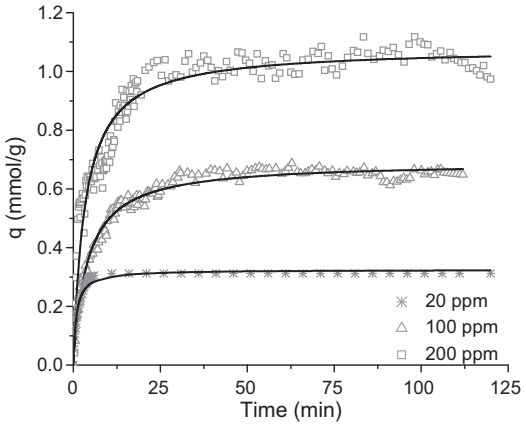

Fig. 1. Kinetics of copper adsorption on APTS-SBA-15-AB at different initial concentrations (Solid lines: model, symbols: experimental data).

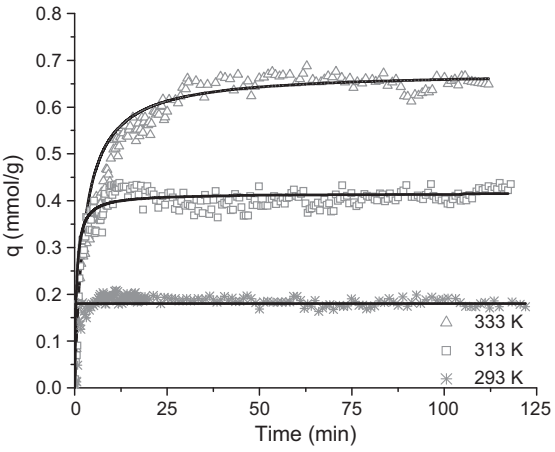

Fig. 2. Kinetics of copper adsorption on APTS-SBA-15-AB at different temperatures (Solid lines: model, symbols: experimental data).

indicating that this mechanism is predominant within this concentration range, i.e. that copper ion occupied two adsorption sites in agreement with literature data for similar adsorbents, including amine-functionalized SBA-15 prepared by grafting [7], amine-functionalized MCM-41 and MCM-48 [15], mesoporous aluminas [3], silica gel [16], and NaX zeolite [13]. Table 1 shows also that the pseudo second-order constants decreased from 6.20 to 0.47 and 0.29 g $mmol^{-1}$ min^{-1} when the initial copper concentration increased from 20 to 100 and 200 mg L^{-1}, respectively. A similar behavior was reported for amine-functionalized SBA-15 prepared by grafting [7], amino-modified silica gel [16], NaX zeolite [13] and rubber leaf powder [14]. Fig. 1 shows that, the maximum adsorption capacity was reached in about 6, 15, and 25 min for initial concentrations of 20, 100, and 200 ppm respectively, indicating very high accessibility of the amine sites to Cu^{2+} adsorption. At the beginning, copper adsorption occurred on the external and most accessible sites. Thus, the initial reaction rate is expected to be high even at low initial concentration since only external diffusion resistance is predominant, while longer reaction time should be required for copper ions to reach less accessible sites. Fig. 1 shows that 6 min was enough to achieve 100% removal of the copper from 20 ppm solution indicating very high efficiency of the adsorbent at low concentration which is a crucial requirement for achieving a viable adsorbent.

3.2. Effect of temperature

The effect of solution temperature was investigated at 293, 313 and 333 K for fixed initial concentration of 100 ppm. Fig. 2 shows that the amount of copper ions adsorbed at equilibrium increases at increasing temperature indicating an overall endothermic process, in agreement with the thermodynamic data reported earlier [11]. Model fitting indicates that the pseudo second-order model provides good correlations for data at all three temperatures. The model constant decreased from 11.79 to 1.96 and 0.47 g $mmol^{-1}$ min^{-1} when temperature increased from 293 to 313 and 333 K, respectively. The decrease in the pseudo first-order and second-order rate constants at increasing temperature is due to the fact that such factors are actually fitting parameters for modeling purposes without being real rate constants. Similar behavior was reported by other workers [17–18].

3.3. Effect of the agitation speed

The agitation speed is an important parameter in any transfer phenomena, since it can promote a certain turbulence which insures a good contact between the phases, a fact which improves the mass transfer. In order to assess the effect of the agitation speed, two different speeds chosen as shown in Fig. 3, where it can be

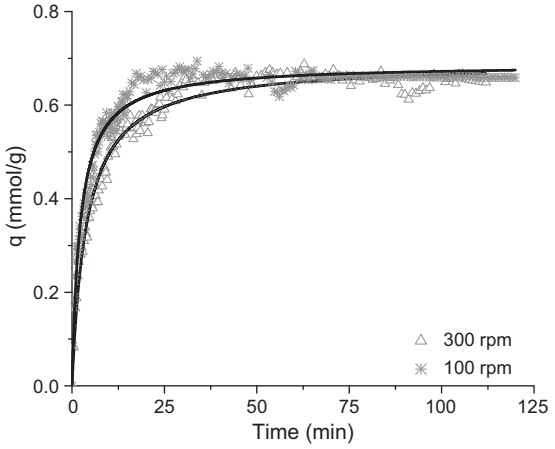

Fig. 3. Kinetics of copper adsorption on APTS-SBA-15-AB at different agitation speeds (Solid lines: model, symbols: experimental data).

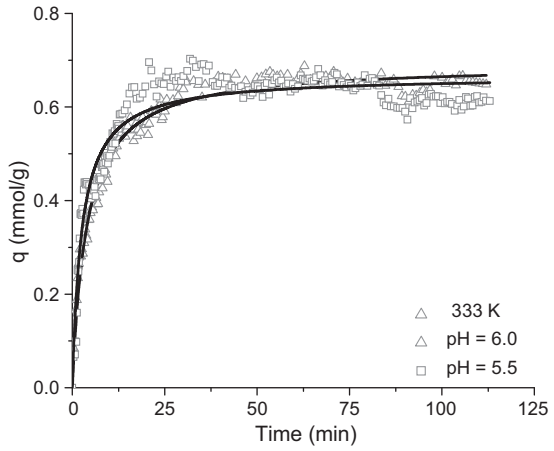

Fig. 4. Kinetics of copper adsorption on APTS-SBA-15-AB at 333 K and different pH (Solid lines: model, symbols: experimental data).

noted that the retention of copper did not change progressively with the agitation speed vs. time, and equilibrium was reached almost in the same time. Therefore it can be concluded that under the current conditions, the agitation speed has no effect on the kinetic performance. This is mainly because for this adsorbent, most of the surface area and therefore the adsorption sites are located within the pores and not on the external surface. Thus, the process is expected to be more dependent on the intraparticle diffusion than the external diffusion. Models fitting shows that at both agitation speeds the kinetics data fit well with the pseudo second-order model with constants of 0.44 and 0.47 g mmol^{-1} min^{-1} for 100 and 300 rpm.

3.4. Effect of pH

Fig. 4 shows that changing the pH of the solution from 5.5 to 6.0 at 333 K resulted in negligible effect on the equilibrium capacity, while the pseudo second-order constant decreased from 2.11 to 0.47 g mmol^{-1} min^{-1}. However, increasing the pH from 6.0 to 6.5 at 293 led to more dramatic changes (Fig. 5). Fig. 5 shows that the adsorption of copper at pH 6.5 was significantly enhanced in comparison to pH = 6 due to the pH effect discussed earlier [11]. Furthermore, at pH 6.5, a period of 40 min was required to reach the equilibrium adsorption capacity (0.58 mmo lg^{-1}), while only two min was required to reach equilibrium (0.18 mmol/g) at pH of 6.0. The value of pseudo second-order constant decreased from 11.79

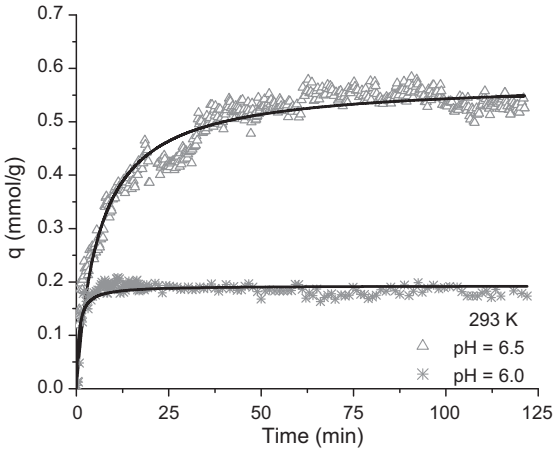

Fig. 5. Kinetics of copper adsorption on APTS-SBA-15-AB at 293 K and different pH (Solid lines: model, symbols: experimental data).

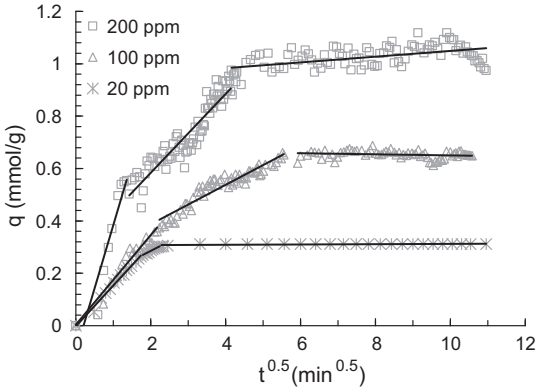

Fig. 6. Intraparticle diffusion plots of copper adsorption onto APTS-SBA-15-AB at different initial concentrations.

to 0.36 g mmol^{-1} min^{-1} when the pH increased from 6.0 to 6.5. A decrease in pseudo second-order constant with increasing the pH was also reported by Öncel [19].

3.5. Intraparticle diffusion

Applying the intraparticle model to the experimental data by plotting q (mmol/g) vs. $t^{0.5}$, Fig. 6 is an illustrative example, shows three distinct stages, as indicated by the solid lines, regarding the rate of change in copper adsorbed: a rapid initial increase, followed by a more gradual increase for about 30 min, followed by a much slower uptake of Cu^{2+}. The initial fast rate is due to the availability of free sites on the external surface and easily accessible sites, in addition to the initial high copper concentration gradient. The rate of adsorption in this stage depends mainly on the external diffusion, thus, as shown in Fig. 6 the higher the concentration, the larger the slope of the solid lines in this region. As time passed, the extent of copper sorption decreased significantly because of the saturation of the external and easily accessible sites as well as the decreasing concentration gradient. Adsorption on sites within the pores takes place. In this stage, copper ions migrate from the bulk of solution to the external surface of the adsorbent followed by diffusion within the pores, which makes the rate slower than in the initial stage. It is obvious that intraparticle diffusion is not the sole rate determining step as the second portion of plots of q versus $t^{0.5}$ did not have zero intercept [14]. The values of k_{id} determined from the slopes of the second stages of the plots are shown in Table 1. Increasing the initial concentration from 20 to 100, then 200 ppm resulted in increasing values of K_{id} from 0.063 to 0.076 and 0.151 mmol/g min$^{0.5}$, respectively as a result of increasing concentration gradient, which is the driving force for diffusion. The same effect was noticed for temperature, the K_{id} increased from 0.036 to 0.048 and 0.076 mmol/g min$^{0.5}$ when the temperature increased from 293 to 313 and 333 K, respectively. At 333 K, the effect of pH on K_{id} was negligible. This is mainly because at this temperature enough energy is supplied to the copper cations to overcome the effect of pH. Moreover, increasing pH from 6 to 6.5 at 293 K led to increasing K_{id} from 0.036 to 0.052 mmol/g min$^{0.5}$ as a result of decreasing the repulsion force between the cations and the surface. The agitation speed had no effect on the kinetics as shown previously with K_{id} of 0.076 and 0.073 mmol/g min$^{0.5}$ at 300 and 100 rpm, respectively. Fig. 6 shows that the second part of the fitted curve for initial concentration of 20 ppm was minimal compared to 100 ppm and 200 ppm indicating the suppressed intraparticle diffusion within the pores. This is mainly because very low concentration of copper may result in Cu^{2+} uptakes below the saturation level of all available amine sites, with Cu^{2+} becoming the limiting reactant leading to adsorption mostly on external sites. It is worth

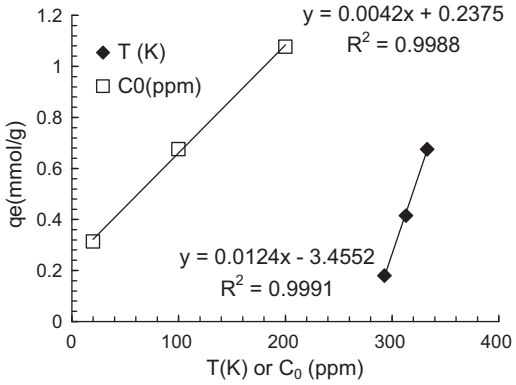

Fig. 7. Equilibrium capacity vs. initial concentration and temperature.

mentioning that the third section of the plots has no kinetic meaning since the material is already saturated. The almost horizontal line corresponds to the equilibrium adsorption capacity, and its intersection with the line of the second section correspond to the time required to achieve equilibrium.

3.6. Predicting the adsorption kinetics

Fig. 7 shows that within the range of initial concentration and temperature used, the equilibrium capacity increased linearly with an increase in C_0 and T according to the following relationships:

$$q_e = 0.0042\,C_0 + 0.2375 \tag{10}$$

$$q_e = 0.0124\,T - 3.4552 \tag{11}$$

The rate constant, and the temperature or the initial concentration are related by Eqs. (12) and (13) as shown in Fig. 8.

$$k_{p2} = 2 \times 10^{11} e^{-0.0805T} \tag{12}$$

$$k_{p2} = 349.47 C_0^{-1.3743} \tag{13}$$

These relationships between q_e (mmol/g), T (K) and C_0 (ppm) as well as k_{p2} (g/mmol min), T (K) and C_0 (ppm) were used in the pseudo second-order kinetic model to develop a general predictive model describing the adsorption kinetics of copper ions on APTS-SBA-15-AB at any initial concentration or any initial temperature and at any time of contact. This approach is valid within the range of validity of Eqs. (10)–(13). From the equations above, the relationships between q, C_0, and T can be represented as:

$$q(T) = \frac{2 \times 10^{11} e^{-0.0805T}(0.0124\,T - 3.4552)^2 t}{1 + 2 \times 10^{11} e^{-0.0805T}(0.0124\,T - 3.4552) t} \tag{14}$$

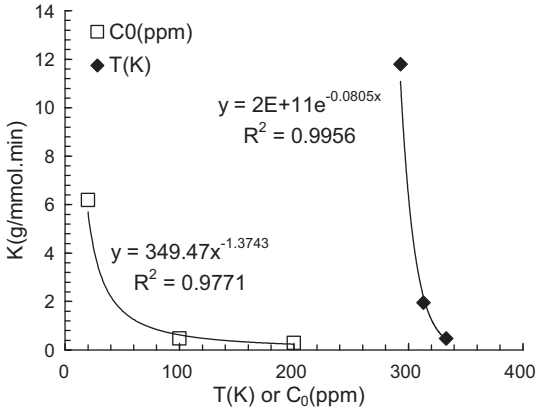

Fig. 8. Pseudo second-order rate vs. initial concentration and temperature.

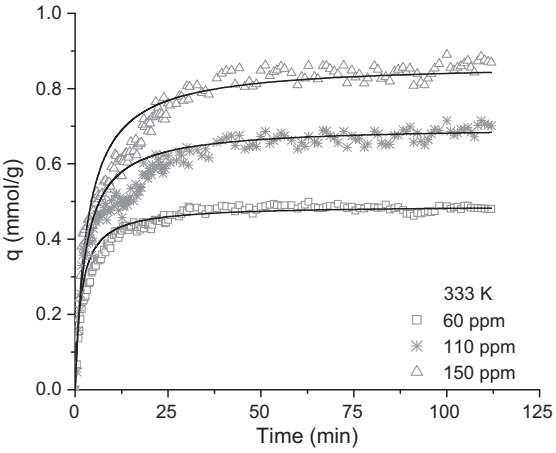

Fig. 9. Validity of the generalized predictive model for different initial copper concentrations (Solid lines: model, symbols: experimental data).

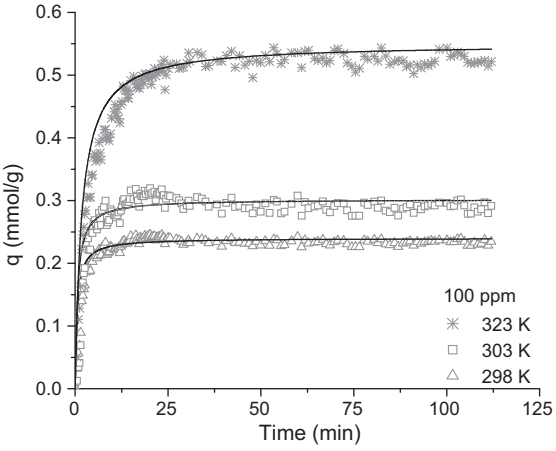

Fig. 10. Validity of the generalized predictive model for different temperatures (Solid lines: model, symbols: experimental data).

$$q(C_0) = \frac{349.47\,C_0^{-1.3743}(0.0042\,C_0 + 0.2375)^2 t}{1 + 349.47\,C_0^{-1.3743}(0.0042\,C_0 + 0.2375) t} \tag{15}$$

These general kinetic models were tested with three different initial concentrations and temperatures as shown in Figs. 9 and 10. The experimental data show an excellent agreement with the data predicted by the general models for the three concentrations and temperatures.

4. Conclusions

Amino-functionalized SBA-15 prepared by co-condensation was used for the removal of copper ions from aqueous solutions. The adsorption capacity and rate were found to be dependent on temperature, pH and initial concentration, while the impact of agitation speed was negligible. The adsorption capacity was favored by increasing initial concentration or temperature. The pH had a beneficial effect at 293 K, but hardly any at 333 K. The pseudo second-order kinetic model provided an excellent fit to the kinetic data. The rate constant decreased with temperature, initial concentration and pH. The intraparticle model showed that the adsorption takes place in three different stages: rapid adsorption controlled by external diffusion, slower adsorption controlled by intraparticle diffusion, and final equilibrium stage. Two general models to predict the kinetic as a function of temperature and initial con-

centration were developed and found to be in excellent agreement with the experimental results.

Acknowledgments

The financial support of the Natural Science and Engineering Council of Canada (NSERC) is acknowledged. A.S. thanks the Federal Government for the Canada Research Chair in *Nanostructured Materials for Catalysis and Separation* (2001–2015).

References

[1] World Health Organization, Guidelines for drinking-water quality: recommendations – Addendum, third edition, vol. 1, 2008.
[2] S. Babel, T.A. Kurniawan, Low-cost adsorbents for heavy metals uptake from contaminated water: a review, J. Hazard. Mater. 97 (2003) 219–243.
[3] S. Rengaraj, Y. Kim, C.K. Joo, J. Yi, Removal of copper from aqueous solution by aminated and protonated mesoporous aluminas: kinetics and equilibrium, J. Colloid Interface Sci. 273 (2004) 14–21.
[4] M. Liu, K. Hidajat, S. Kawi, D.Y. Zhao, A new class of hybrid mesoporous materials with functionalized organic monolayers for selective adsorption of heavy metal ions, Chem. Commun. (2000) 1145–1146.
[5] L. Zhang, C. Yu, W. Zhao, Z. Hua, Hi Chen, L. Li, J. Shi, Preparation of multi-amine-grafted mesoporous silicas and their application to heavy metal ions adsorption, J. Non-Cryst. Solids 353 (2007) 4055–4061.
[6] y. Jiang, Q. Gao, H. Yu, Y. Chen, F. Deng, Intensively competitive adsorption for heavy metal ions by PAMAM-SBA-15 and EDTA-PAMAM-SBA-15 inorganic-organic hybrid materials, Microporous Mesoporous Mater. 103 (2007) 316–324.
[7] J. Aguado, J.M. Arsuaga, A. Arencibia, M. Lindo, V. Gasco'n, Aqueous heavy metals removal by adsorption on amine-functionalized mesoporous silica, J. Hazard. Mater. 163 (2009) 213–221.
[8] J. Aguado, J.M. Arsuaga, A. Arencibia, Influence of synthesis conditions on mercury adsorption capacity of propylthiol functionalized SBA-15 obtained by co-condensation, Microporous Mesoporous Mater. 109 (2008) 513–524.
[9] J. Aguado, J.M. Arsuaga, A. Arencibia, Adsorption of aqueous mercury (II) on propylthiol-functionalized mesoporous silica obtained by cocondensation, Ind. Eng. Chem. Res. 44 (2005) 3665–3671.
[10] M.C. Bruzzoniti, A. Prelle, C. Sarzanini, B. Onida, S. Fiorilli, E. Garrone, Retention of heavy metal ions on SBA-15 mesoporous silica functionalised with carboxylic groups, J. Sep. Sci. 30 (2007) 2414–2420.
[11] E. Da'na and A. Sayari, Adsorption of copper on amine-functionalized SBA-15 prepared by co-condensation: Equilibrium properties, Chem. Eng. J. (in press) doi:10.1016/j.cej.2010.11.016.
[12] A. Walcarius, C. Delacôte, Rate of access to the binding sites in organically modified silicates. 3. Effect of structure and density of functional groups in mesoporous solids obtained by the co-condensation route, Chem. Mater. 15 (2003) 4181–4192.
[13] S. Svilovic, D. Rusic, R. Stipisic, Modeling batch kinetics of copper ions sorption using synthetic zeolite NaX, J. Hazard. Mater. 170 (2009) 941–947.
[14] W.S. Wan Ngah, M.A.K.M. Hanafiah, Adsorption of copper on rubber (Hevea brasiliensis) leaf powder: kinetic, equilibrium and thermodynamic studies, Biochem. Eng. J. 39 (2008) 521–530.
[15] A. Benhamou, M. Baudo, Z. Derriche, J.P. Basly, Aqueous heavy metals removal on amine-functionalized Si-MCM-41 and Si-MCM-48, J. Hazard. Mater. 171 (2009) 1001–1008.
[16] V. Manu, M. Haresh, C.B. Hari, V.J. Raksh, Adsorption of Cu^{2+} on amino functionalized silica gel with different loading, Ind. Eng. Chem. Res. 48 (2009) 8954–8960.
[17] M. Mohammad, S. Maitra, N. Ahmad, A. Bustam, T.K. Sen, B.K. Dutta, Metal ions removal from aqueous solution using physic seed hull, J. Hazard. Mater. 179 (2010) 363–372.
[18] M.H. Kalavathy, L.R. Miranda, Comparison of copper adsorption from aqueous solution using modified and unmodified Hevea brasiliensis saw dust, Desalination 255 (2010) 165–174.
[19] M.S. Öncel, Adsorption of copper (II) from aqueous solution by Beidellite, Environ. Geol. 55 (2007) 1767–1775.